Materials Letters 263 (2020) 127248

Contents lists available at ScienceDirect

Materials Letters

journal homepage: www.elsevier.com/locate/mlblue

$Ca_3MgSi_2O_8$: Novel low-permittivity microwave dielectric ceramics for 5G application

Hadi Barzegar Bafrooei [a,b,*], Bing Liu [a], Weitao Su [c], Kai Xing Song [a,*]

[a] College of Electronic Information and Engineering, Hangzhou Dianzi University, Hangzhou, China
[b] Department of Materials Science and Engineering, School of Engineering, Meybod University, Yazd, Iran
[c] College of Materials Sciences and Environmental Engineering, Hangzhou Dianzi University, Hangzhou, China

ARTICLE INFO

Article history:
Received 17 October 2019
Received in revised form 23 December 2019
Accepted 23 December 2019
Available online 24 December 2019

Keywords:
Low permittivity
Dielectrics
Ceramics
Synthesis and sintering
5G

ABSTRACT

In this research, the novel low permittivity $Ca_3MgSi_2O_8$ microwave dielectric ceramics have been fabricated via conventional solid state process and their synthesis, sintering and microwave dielectric properties were investigated. The thermal behavior of the ball milled stoichiometric mixtures was investigated using simultaneous thermal analysis. Scanning electron microscopy image and particle size distribution of synthesized powder showed that the particle size fell into a range of ~1–11 μm. X-ray diffraction analysis of synthesized and sintered ceramics showed that single phase $Ca_3MgSi_2O_8$ crystallized in a monoclinic structure. Relative density near 99% of theoretical density, ε_r = 13.8, quality factor ($Q \times f$) ~ 27000 GHz (at 10.8 GHz) and $\tau_f = -62$ were obtained for ceramics sintered at 1375 °C. Hence, it is to be hoped that $Ca_3MgSi_2O_8$ ceramics can be selected as a possible candidate for 5G application and their performance can be improved by optimization of synthesis and sintering process.

1. Introduction

During the last few years, microwave dielectric ceramics with suitable ε_r, high $Q \times f$ value and near-zero temperature coefficient of resonant frequency (τ_f) have been intensively investigated as the key components for microwave substrates, resonators, oscillators, etc. Moreover, the great explosion of information and the rapid development of wireless communications since entering the 21st century have put forward higher and newer demands for the development of microwave dielectric ceramics. To meet the emerging requirements, exploring the upper limit of dielectric properties and searching for new low-loss candidates (for 5G technology) have increasingly become the focus of academic attention. For 5G, both low permittivity (ε_r < 15) and low loss (high quality factor) are essential due to high data transmission rate can only be achieved by low time delay signal transmission used in high frequency communications which will facilitate the internet of things and integrated urban transportation networks of self-drive vehicles [1,2].

It is well known that silicate based ceramics are promise candidates for the high frequency application due to low permittivity and loss [3]. In recent years, several silicate based microwave ceramics such as $MgAl_2Si_5O_{18}$ [4], Mg_2SiO_4 [5] and $CaMgSiO_4$ [6] have been reported for application of low permittivity device. The monoclinic $Ca_3MgSi_2O_8$ with space group P21/a is one of the low cost practical ceramics that belongs to Ca-Mg-Si-O system. Although the luminescence [7] and bio-properties [8] of $Ca_3MgSi_2O_8$ compounds have been investigated, but there have been no reports on the microwave dielectric properties of $Ca_3MgSi_2O_8$ ceramics so far.

The aim of this research is to address the microwave dielectric properties $Ca_3MgSi_2O_8$ ceramics for 5G applications. In this research we report successful synthesis and sintering of Merwinite ceramics and their microwave dielectric properties.

2. Experimental procedure

The $Ca_3MgSi_2O_8$ ceramics were fabricated via conventional solid state method using $CaCO_3$ (99.5%), MgO (99.9) and SiO_2 (99.5%) as the raw materials. Stoichiometric of starting materials were ball milled in ethanol for 4 h and then calcined at 1250 °C in air for 4 h to synthesized pure phase with monoclinic structure. Then calcined powders were re-milled with 5 wt% PVA solution, pressed into cylindrical pellets under a uniaxial pressure 200 MPa. The pellets were sintered at 1300–1400 °C in air for 3 h.

* Corresponding authors at: College of Electronic Information and Engineering, Hangzhou Dianzi University, Hangzhou, China.
E-mail addresses: hadi.barzegar@meybod.ac.ir, hadi@hdu.edu.cn (H.B. Bafrooei), kxsong@hdu.edu.cn (K.X. Song).

https://doi.org/10.1016/j.matlet.2019.127248
0167-577X/

The thermal behavior of the reaction ball milled initial mixture was studied using combined simultaneous thermal analysis (TG-DTA, NETZSCH STA) up to 1350 °C in air, with a heating rate of 600 °C h^{-1}. Crystal structure and phase identification of synthesized and sintered ceramics were analyzed using X-ray diffraction (XRD: RIGAKU D/max 2550/PC, Rigaku Co., Tokyo, Japan). The particle size distribution of synthesized powder after milling procedure for 4 h was measured by Mercury Intrusion porosimeter (Autopore IV9500, Micromeritics, USA). The Raman spectra were obtained using a Renishaw in via Raman Microscope at room temperature. Bulk density was measured by Archimedes method. Morphology characterization of synthesized powder and microstructure of thermally etched surfaces of sintered specimens were observed by a scanning electron microscope (SEM: SIRION-100, FEI Co., Eindhoven, Nederlands). The evaluations of microwave dielectric properties were performed in the frequency range of 10–11 GHz using a vector network analyzer (E8363B, Agilent Technologies Inc., Palo Alto, CA). The quality factor was measured using the resonant-cavity method and ε_r and τ_f were also measured using Hakki-Coleman method. The τ_f value was measured in the temperature range from 20 °C to 80 °C and was calculated as following formula:

$$\tau_f = \frac{f_{80} - f_{20}}{f_{20} \times (80 - 20)} \times 10^6 (\mathrm{ppm/^\circ C})$$

where, f_{20} and f_{80} denoted the resonant frequencies at 20 °C and 80 °C, respectively.

3. Results and discussion

The simultaneous thermogravimetric and differential thermal analysis (TG/DTA) were performed on $3CaCO_3$-MgO-$2SiO_2$ initial mixture powders that were ball milled for 6 h in the temperature range of 25–1350 °C. Fig. 1a show the TG/DTG/DTA curves of ball milled powder. According to TG/DTG curves, the weight loss of the initial mixture powders can be divided into three distinct stages. The first and second stages are appeared between 250–350 °C and 450–550 °C, which can be attributed to evaporation of water and the hydration of the chemically absorbed water molecules, respectively. These mass losses are accompanied by small endothermic peaks in the DTA curves at 290 °C and 520 °C. The third stage, which is associated with remarkable weight loss, occurs in the range of 580–760 °C probably due to the decomposition of calcium carbonate that is accompanied by endothermic peak in DTA curve at 730 °C. The exothermic reactions occurs in a temperature range of 1000–1250 can be attributed to the intermediate phases and final merwinite phase formation.

The room temperature powder XRD pattern of synthesized and sintered $Ca_3MgSi_2O_8$ samples in 1250 °C and 1375 °C, respectively, are shown in Fig. 1(b). The XRD pattern of synthesized powder shows that the reaction between starting materials seems to be completed at 1250 °C. All of the synthesized and sintered diffraction patterns can be successfully indexed according to monoclinic phase $Ca_3MgSi_2O_8$ (JCPDS #1-074-0382, space group #P21/a). As expected, no secondary phase is detected in the synthesized and sintered ceramics in the sensitivity limit of X-ray diffraction apparatus.

Fig. 2(a) shows the SEM image of synthesized powder at 1250 °C for 4 h. it is clearly observed that particles containing irregular morphology and the size of particles were within the range of submicrometer to ~10 μm. It can be obviously seen that most particles are smaller than 7 μm. For further characterization, the particle size distribution was studied. As shown in Fig. 2(b), the particle size distribution of synthesized powder fell into a range of ~1–11 μm. The values corresponding to 10, 30, 50, 70 and 90 (d_{10}, d_{30}, d_{50}, d_{70} and d_{90}) of the cumulative size distribution are collected in table as an inset. The average particle size d_{50} powders were about 3.8 μm. the particle size distribution results are in agreement with the SEM powder micrograph.

The Raman spectra for sintered ceramic in the frequency region, 50–1000 cm^{-1}, are shown in Fig. 2(c). The high frequency bands exist in the broad range of 700–1000 cm^{-1} and weak bands in moderate frequency between 500 and 600 cm^{-1} are corresponding to the υ stretching vibration and δ bending vibration mode of SiO_4 tetrahedron [9]. In addition, peaks at low frequency in the range of 400–450 cm^{-1} and 100–350 indicated the vibration mode of Ca-O and Mg-O bonds [10].

Fig. 3a illustrates linear shrinkage and relative density evolution of the sintered $Ca_3MgSi_2O_8$ pellets as a function of sintering temperature. The shrinkage and relative density values of sintered ceramics increased from 8.2 to 12.8% and 92 to 99%, respectively, as sintering temperature increased from 1300 to 1375 °C and thereafter saturated, approximately. The increase in shrinkage and relative density can be attributed to the decrease of porosity accompanied by an increase in grain growth.

The inset image of Fig. 3a presented surface morphology $Ca_3MgSi_2O_8$ ceramics sintered in optimum sintering temperature. It can be obviously seen that a full densified microstructure with distinct and clean grain boundaries and grains size about 3–15 μm was developed in the ceramics sintered at 1375 °C.

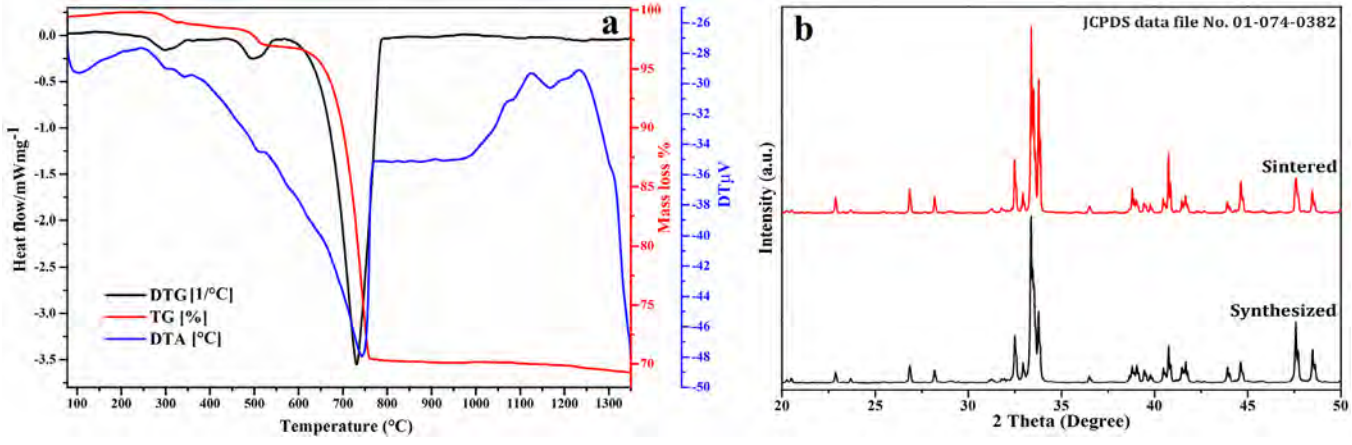

Fig. 1. a) STA curves of the ball milled mixtures, b) XRD patterns of synthesized powder and sintered ceramic.

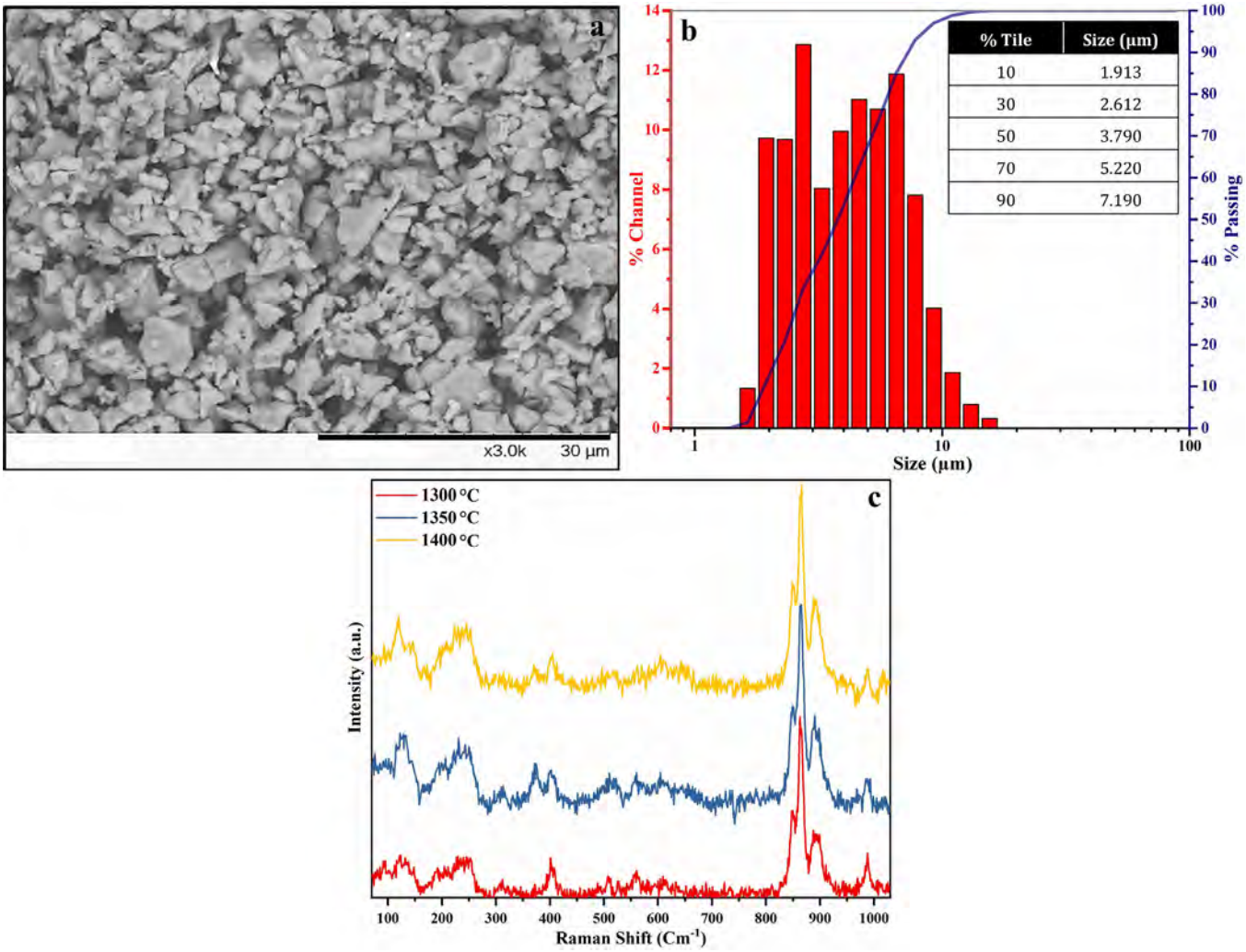

Fig. 2. a) SEM image and b) particle size distribution of synthesized powder, c) Raman Spectra of sintered ceramics.

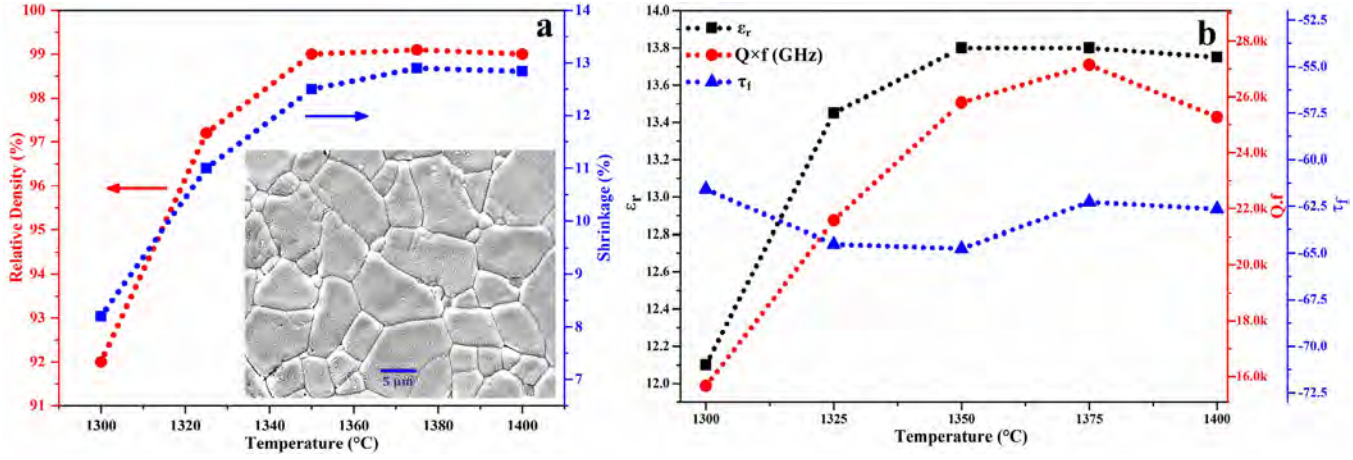

Fig. 3. a) Relative density, linear shrinkage and SEM Image sintered ceramics, b) microwave dielectric properties of sintered ceramics.

Fig. 3b plots the variation tendencies of the microwave dielectric properties of $Ca_3MgSi_2O_8$ ceramics as a function of sintering temperature. Similar trend to the relative density can be seen, which implies constant dielectric and Q × f of $Ca_3MgSi_2O_8$ can mainly attributed to densification and grain growth. It is observed that the maximum ε_r value being 13.8, was achieved for ceramics sintered at 1375 °C. On the other hand, the observed improvement in the Q × f value as function of sintering temperature could be

attributed to the increase of density and grain growth in $Ca_3MgSi_2O_8$ ceramics. The maximum Q × f value of 27,000 GHz was obtained at 1375 °C. As shown in Fig. 3b, it can be seen that τ_f is not sensitive to the sintering temperature and it changes from −61.6 to −64.7 ppm/°C. This is mainly due to the fact that no chemical composition changed happened during sintering process. Further improvement in microwave dielectric properties is possible by optimization of synthesis and sintering processing as well as engineering of structure and microstructure.

4. Conclusions

In conclusion, we have been successful in synthesizing and sintering the single phase monoclinic $Ca_3MgSi_2O_8$ ceramics. XRD and Raman Analysis revealed that $Ca_3MgSi_2O_8$ samples demonstrate a monoclinic structure. STA results showed that monoclinic phase formation occurs at temperature above 1200 °C. the particle size of synthesized powders was in the range of 1–11 μm. Excellent microwave dielectric characteristics for the samples sintered at 1375 °C: ε_r = 13.8, Q × f ~ 27000 GHz and τ_f = −62 ppm/°C were achieved using conventional solid state reaction process, exhibiting a potential for high frequency applications. Our results confirmed the as-synthesized and sintered $Ca_3MgSi_2O_8$ microwave dielectric ceramics are inexpensive materials for 5G application.

CRediT authorship contribution statement

Hadi Barzegar Bafrooei: Conceptualization, Project administration, Writing - original draft, Writing - review editing. **Bing Liu:** Methodology, Writing - review editing. **Weitao Su:** Software, Data curation. **Kai Xing Song:** Supervision, Writing - review editing.

Declaration of Competing Interest

The authors declare that they have no known competing financial interests or personal relationships that could have appeared to influence the work reported in this paper.

References

[1] I.M. Reaney, D. Iddles, Microwave dielectric ceramics for resonators and filters in mobile phone networks, J. Am. Ceram. Soc. 89 (7) (2006) 2063–2072, https://doi.org/10.1111/j.1551-2916.2006.01025.x.
[2] W.J. Sun, W.W. Yang, P. Chu, J.X. Chen, A wideband stacked dielectric resonator antenna for 5G applications, Int. J. RF Microw. Comput. Aided Eng. (2019), https://doi.org/10.1002/mmce.21897 e21897.
[3] J. Wei, P. Liu, H. Lin, Z. Ying, P. Zheng, W. Su, K.X. Song, H. Qin, Crystal structure and microwave dielectric properties of CaTiO3 modified $Mg_2Al_4Si_5O_{18}$ cordierite ceramics, J. Alloys Compd. 689 (2016) 81–86, https://doi.org/10.1016/j.jallcom.2016.07.119.
[4] M. Terada, K. Kawamura, I. Kagomiya, K. Kakimoto, H. Ohsato, Effect of Ni substitution on the microwave dielectric properties of cordierite, J. Eur. Ceram. Soc. 27 (2007) 3045–3048, https://doi.org/10.1016/j.jeurceramsoc.2006.11.050.
[5] K.X. Song, X.M. Chen, Phase evolution and microwave dielectric characteristics of Ti-substituted Mg_2SiO_4 forsterite ceramics, Mater. Lett. 62 (2008) 520–522, https://doi.org/10.1016/j.matlet.2007.05.078.
[6] H. Zhou, J. Huang, X. Tan, G. Fan, X. Chen, H. Ruan, Microwave dielectric properties of low-permittivity $CaMgSiO_4$ ceramic, J. Mater. Sci.: Mater. Electron. 28 (2017) 15258–15262, https://doi.org/10.1007/s10854-017-7405-5.
[7] P. Dewangan, D.P. Bisen, N. Brahme, S. Sharma, Structural characterization and luminescence properties of Dy^{3+} doped $Ca_3MgSi_2O_8$ phosphors, J. Alloys Compd. 777 (2019) 423–433, https://doi.org/10.1016/j.jallcom.2018.10.390.
[8] A. Nadernezhad, F. Moztarzadeh, M. Hafezi, H. Barzegar-Bafrooei, Two step sintering of a novel calcium magnesium silicate bioceramic: sintering parameters and mechanical characterization, J. Eur. Ceram. Soc. 34 (2014) 4001–4009, https://doi.org/10.1016/j.jeurceramsoc.2014.05.014.
[9] C. Fredericci, E.D. Zanotto, E.C. Ziemath, Crystallization mechanism and properties of a blast furnace slag glass, J. Non-Cryst. Solids 273 (2000) 64–75, https://doi.org/10.1016/S0022-3093(00)00145-9.
[10] A.G. Kalampounias, IR and Raman spectroscopic studies of sol–gel derived alkaline-earth silicate glasses, Bull. Mater. Sci. 34 (2011) 299–303, https://doi.org/10.1007/s12034-011-0064-x.